Audio Engineering Society

Convention Paper

Presented at the 123rd Convention
2007 October 5–8 New York, NY, USA

Scattering uniformity measurements and first reflection analysis in a large non-anechoic environment.

Lorenzo Rizzi[1], Angelo Farina[2], Paolo Galaverna[3], Paolo Martignon[1], Andrea Rosati[1] and Lorenzo Conti[1]

[1] LAE - Laboratorio di Acustica ed Elettroacustica, Parma, Italy
rizzi@laegroup.org ; martignon@laegroup.org ; rosati@laegroup.org ; conti@laegroup.org

[2] Dipartimento di Ingegneria Industriale, Università di Parma, Italy
farina@unipr.it

[3] Genesis Acoustic Workshop, Parma, Italy
p.galaverna@genesis-aw.com

ABSTRACT

A new campaign of experiments was run on the floor of a large room to obtain a long enough anechoic time window: this permitted to study the first reflection from the panels themselves and their diffusion uniformity. The results are discussed, comparing them with past measurements and with the ones from a simplified set-up with a smaller geometry. Some key matters to measurement are discussed, they were proposed in a recent comment letter posted to the specific AES-4id document committee on its reaffirmation. An analysis of the single reflection and reflectivity data was undertaken to investigate the behavior of a perforated panel and the measurement set-up overall potential.

1. INTRODUCTION: THEORETICAL AND EXPERIMENTAL SET-UP

A new campaign of scattering measurements was undertaken between September and October 2006, to continue the first one executed on single panels in the previous month of April and discussed in October at the AES convention in San Francisco [1]. The AES recommendation document 4id-2001 [2] and Cox and D'Antonio's [3, 4] previous papers on the matter were used as reference to start the study.

This time mostly pairs of panels were considered, to investigate the phenomena of uniform geometric diffusivity in more realistic situations. The first campaign's main target was also to compare this type of

analysis with a 1999 Italian study on single panels [5, 6].

In April 2007 the authors proposed some modifications and questions to the AES document reaffirmation [7] which discussion was accepted but postponed for lack of time.

All the data from the first campaign investigations on single panels reflection from a smaller measurement set-up were also elaborated, to search for focusing effects and to compare the results from larger scale studies.

The article discusses the results obtained on a limited number of measurements, giving some new insights and pointing out new directions of research. It expands the first analysis that was partially presented by the authors at ICA 2007 in Madrid [8].

1.1 Experimental set-ups.

As stated in the AES document annex A.2.2, the anechoic conditions for studying the panels' first reflection were obtained by setting the microphone array, the source and the panel itself on the floor of a very large industrial shed which is normally used for fairs and exhibitions.

This was the same ground of the past research and it had been already considered valid to avoid room reflections to corrupt the one under study. The measurement ground was larger than the minimum required volume of 18.2 x 23.6 x 9 meters of height, specifically re-calculated for a 10 msec long anechoic time window.

This setup is ideal to study single plane (anisotropic) diffusers and to actually characterize the first reflection geometry in the cylindrical emi-space in front of them.

1.1.1. Standard geometry setup.

The receiver array had a semicircular disposition as requested by the concept of uniform diffusivity, it had the suggested, standard radius of 5 meters, centered at the panels' frontal face vertical axis base. The source was moved along a 10 meter semicircle centered as the smaller one.

Studying April's results, it was decided to investigate 5 source positions for each double panel assembly (-60°,-30°, 0°, 30° 60° incidence – which had showed to be a good choice in approximating the full measurement averaging 18-incidence angles) and 3 for each single panel, as suggested for a fast acquisition by the AES recommendation which asks to use –55°, 0°, 55° of incidence – circles in a lighter colour in figure 1). Every source and panel movement was man operated.

Since only 60 x 60 cm panels were considered, when the analysis took two panels at the time it created a surface roughly 120 cm wide per 60 cm high.

The choice of using 24 receivers was also taken from the past research results which showed little difference with 48 channel ones, permitting faster acquisitions on hardware potential.

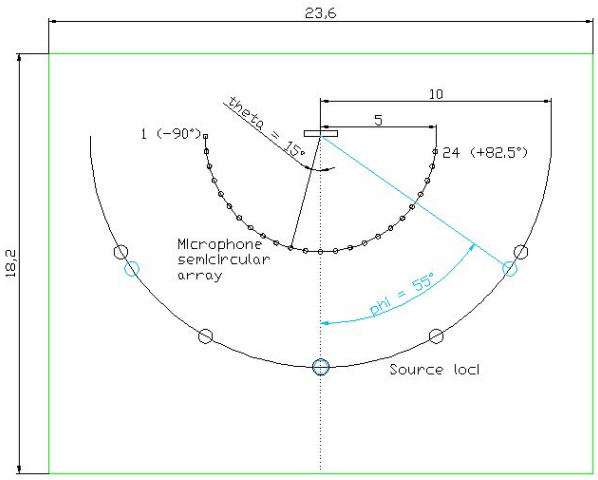

Figure 1

1.1.2. Smaller geometry setup.

A smaller geometry was used in April 2006, to start a study of the phenomenon from a closer point of view through a simpler setup.

7 microphones were set on a R = 1 meter radius circular arc, covering a 120° span with a 15° resolution. The source was set at 2 meters from the panel and moved on a larger circular arc on 5 angles of incidence (-55°, -20°, 0°, 20°, 55° - Figure 2 shows normal incidence).

This geometry permits investigations on a much smaller space (5.9 x 4.9 x 2.4 m of height), smaller of the average room of civil use in Italy. It is important to remember that in this case the usable anechoic window cannot be larger than 5.5 msec, since the first strong spurious reflection, coming from the source itself, always arrives at 2*R/c seconds after the direct arrival:

in this case 2 meters, after the panel's first reflection under study.

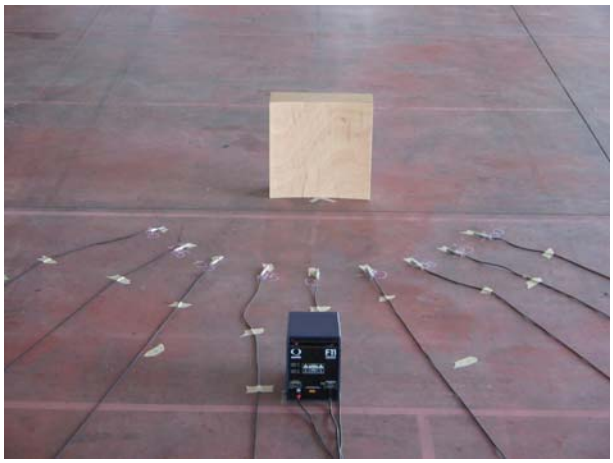

Figure 2.

1.2 Acquisition process and protocol.

The measurement hardware was made by:

- 24 Bruel&Kjaer 4188 microphones with 2671 preamplifiers (phantom-powered);
- 3 8-channels Behringer AD-DA 8000 Converters;
- 1 RME Hammerfall DIGI9652 soundcard;
- 1 Turbosound TQ440 sound source for the standard geometry measurements
- 1 Quested F11 sound source for the smaller geometry measurements.

The impulse responses were taken using the sine sweep technique [9]: a logarithmic sine sweep was generated using the Aurora Adobe Audition plug-ins (www.aurora-plugins.com). The signal ranged between 50 and 10000 Hz, lasted 10 seconds and had a 5 seconds silence interval at the end. In the past measurements this method was demonstrated to be faster than the otherwise proposed MLS method (it does not need averaging on multiple measures) and to be good to reject the existing background noise from the nearby A1 national toll way.

A key factor from the past campaign was optimising the measurement protocol itself: this time a 24 single channel recording was executed through Adobe Audition to quicken Matlab elaborations in the digital processing phase.

Also, it was decided to measure all of the panels with the same incidence angle within a short time gap, comprising the empty take (done to acquire h2 as explained in the next paragraph), this guaranteed a large correlation between them.

A few measurements had to be repeated because of an acquisition fault, this lost perfect correlation between h1 and h2 : a remedy was hence developed for the matter.

1.3 Data processing.

As requested by the sine sweep method, the impulse responses were obtained by convolving the recorded sine sweeps (the room sine sweep response) with a previously saved inverse sine sweep and by properly windowing in time.

For every sound incidence angle and type of panel a 24 channel response (h_1) and a single 24 channel response with no panel present (h_2) was obtained and stored for each angle of incidence: the second one was recorded once and considered for all of the panels recorded at every incidence angle. Every half day the measurement system response was measured (h_3) as specified.

As required by the AES document the single reflection response is obtained by subtracting the two impulse responses h_1-h_2, this rejects most of the direct wave and spurious reflections. The actual reflection (h_4) is then found by deconvolving the system response by division in the frequency domain:

$$h_4 = IFT\left[\frac{FT[h_1 - h_2]}{FT[h_3]}\right] \quad (1)$$

The first two impulse responses must be time windowed at the first reflection arrival: the time window start was initially decided by visual inspection as suggested.

After division in the frequency domain, a frequency window was applied to the data, to cut out all of the high frequency discrepancies due to time windowing, this operation was considered necessary after inspection of the single tracks.

At this point the H_4 (FFT(h_4)) absolute values where squared and summed strictly within each third octave and octave frequency band limits for each microphone, obtaining the required L_i (referring to the third octave

band pseudo-intensity value at the i-th microphone of N) .

Then these values were used to obtain the angular dependent (φ – angle of sound incidence) uniform diffusivity coefficients (equation 2), the random incidence ones (as the average on all of the investigated incidences) and to plot the energetic polar graphs in a dB scale (figure 3 shows the Gal2 pair first reflection geometry when sound is incising from 60° in the 6 frequency bands under study).

$$d_{\varphi} = \frac{\left(\sum_{i=1}^{N} 10^{L_i/10}\right)^2 - \sum_{i=1}^{N}\left(10^{L_i/10}\right)^2}{(N-1)\sum_{i=1}^{N}\left(10^{L_i/10}\right)^2} \quad (2)$$

The uniform diffusion coefficient under study is a qualitative parameter: it gives a value of 1 to a panel which reflects the same amount of energy in all directions (the ideal scatterer) and 0 to the totally specular reflective panel (only one narrow angle of reflection).

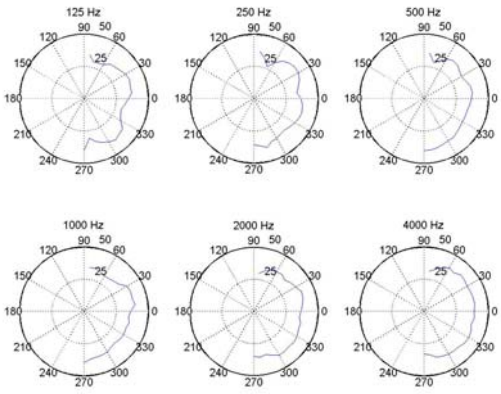

Figure 3.

2. DATA PROCESSING OPTIMISATION.

2.1 Track re-alignment by correlation verification.

In the few measurements where h_2 had to be measured a second time, at a time interval larger than a few minutes from h_1 there was always a small incorrelation between the respective tracks.

Re-alignment was hence obtained by cross-correlating each track pair and looking for the maximum position respect to the single tracks double length. Figure 4 shows the effect of this process on a single track subtraction (h_1(4th mic) - h_2(4th mic)): the lower one is actually smoother and shows less high frequency energy.

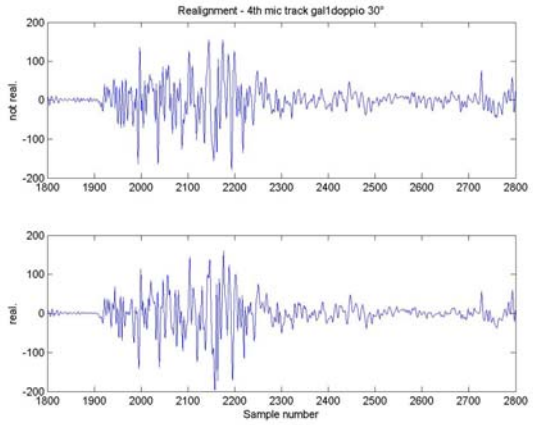

Figure 4.

The following graph shows the method application effect on the overall uniform diffusion coefficient under study: the random coefficient d for the two coupled panel backs is smoother in frequency to a more realistic trend and has smaller values, expecially at high frequencies.

This experience demonstrates the importance of defining in more detail a procedural protocol for the execution of the measurements in the recommendation document, expecially in the annex part regarding measurements in virtually anechoic spaces as the one considered for this study.

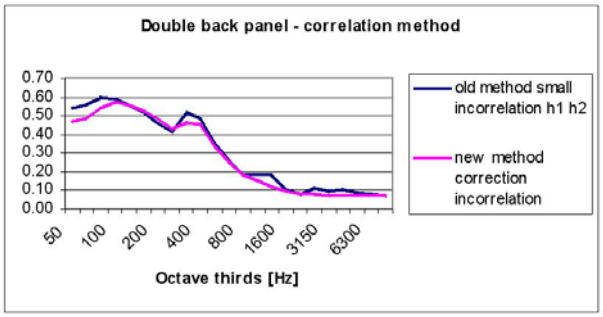

Figure 5.

2.2 Differentiated time window.

A 500 samples time window (10 msec) was considered as in all of the past experiments, to avoid any influence from the first room reflections (from objects hung at the ceiling of the industrial shed).

The window's edges were smoothed through a raised cosine roll-on and roll-off and it started roughly 35 samples before the expected reflection arrival. This avoided high frequency oscillations that are typical of rectangular time windowing.

As stated by the recommendation document the reflected wave arrival can be predicted through a simple geometrical model, this means setting two point sources at the panel border angles. This model works very well for shoe-box shaped ones where the reflected and direct wave arrivals can be easily predicted:

$$r_{reflected} = \min[\sqrt{(2r\cos\varphi)^2 + (2\sin\varphi \mp x)^2} + \sqrt{(r\cos\theta)^2 + (r\sin\theta \pm x)^2}\,] \quad (3)$$

$$r_{direct} = \sqrt{r(1 - 2\cos^2\theta + 2\sin\varphi + 2\cos\varphi)} \quad (4)$$

r is the receiver semicircle radius and the distance between the source and the semicircle
x is half the panel's width
θ is the angle of observation.
φ is the angle of sound incidence on the panel

Superposing these theoretical curves with sonar-like measurement surface graphs of h_1-h_2 (each track subtraction is plotted on a vertical line in the graph) there is a very good matching.

Figure 6 shows the result on double panel-back (reference panel) measurements with normal incidence, where the lower red curved line represents the shorter path of the two profiles of equation 3, the blue upper line is the longest (coming from the most distant edge respect to the microphone) and the black horizontal line is the ideal reflection from a perfect semi-cylindrical panel.

The figure demonstrates a perfect match between theoretical and measured values. It validates the 'border effect' model of introducing point sources on the panel's edges as a definite marker of the beginning of the reflection phenomena. It is also important to note that inside the specular region (in this case in the three central microphones) the reflection is actually ideal.

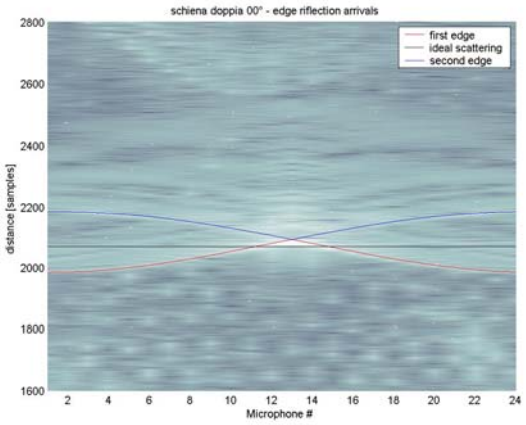

Figure 6.

The sonar-like plot, originally mutuated from Wave Field Analysis studies, demonstrates to be a very good instrument in studying and verifying the measurements' data in all of the elaboration phases, up to the time windowing one.

In the past campaign the time window was quickly set by looking for the closest reflection and imposing the same beginning to all of the 24 tracks. The present study actually permits to make the reflection recognition automatic and later to align the tracks to optimize the division with h_3 which can be windowed using the same concepts (length, beginning, etc.).

The main advantage of the use of this method is procedural speed and low energy retrieval, as expected by better centered windows (figure 7). All the

subsequent analysis used both the two methods when necessary.

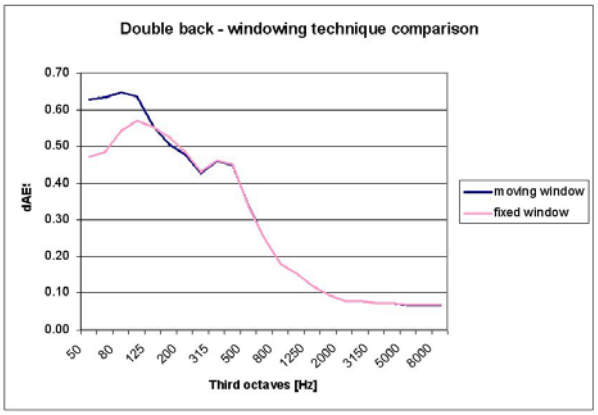

Figure 7.

3. DIFFUSION UNIFORMITY RESULTS.

3.1 Comparing the two observation geometries' results.

3.1.1. Focusing investigation.

The smaller geometry measurement setup was firstly intended to investigate focusing effects as shortly suggested by the AES recommendation document (paragraph 4.2). As seen in figure 2 a cylindrical-parabolic panel was built to study a well known response, its geometrical focus was designed right in front of its vertex at a 1 m distance.

The following polar graphs compare the reflection geometry of the parabolic panel (upper figure) with the reference panel one (lower figure) when sound is incising from –55°: above 500 Hz there is a slight asymmetry near the 0° direction that can be related to the focusing effect .

The results actually appear feeble because of the poor angular resolution of the microphone array: further analysis is required to confirm this setup potential and verify time-truncation effects linked to its dimensions.

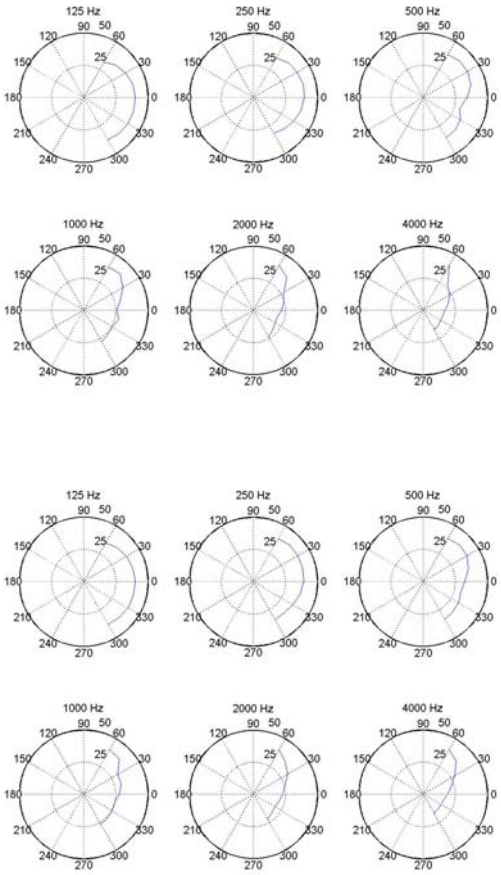

Figure 8a, 8b

3.1.2. Coefficient results.

The calculated uniformity coefficient values on the small geometry are clearly correlated with the larger scale measurements undertook in April 2006 on the same single panels [1].

The following graphs (figure 9) show a similar trend within and between the same panel's types, the difference in coefficient value in modulus supports the well known measurement system dependence on its geometry.

Again, further research is still needed, because the smaller setup has theoretical and practical limitations (partially explained in the recommendation document's first paragraphs and in point 1.1.2 of this article).

But it has still the quite appealing advantage to require average sized rooms for measurements.

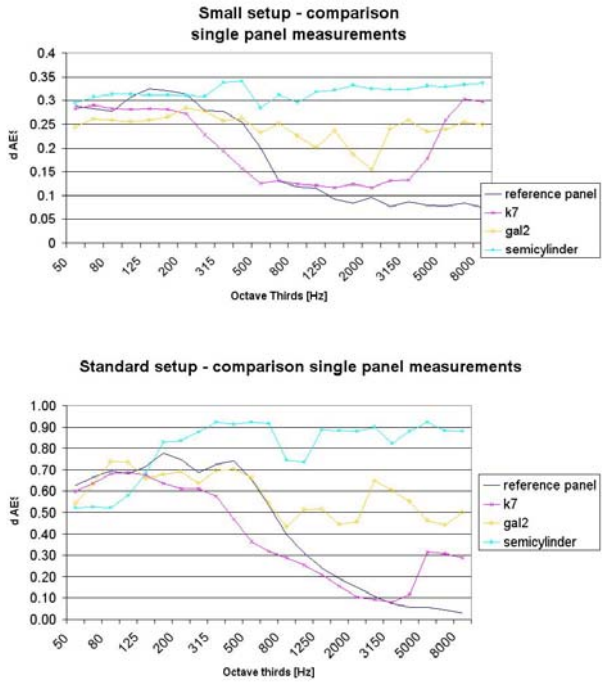

Figure 9a, 9b.

3.2 Panel pairs' results.

These study was intended to conclude April's investigations [1] on single panels of the same typology with a more realistic situation.

3.2.1 Reference flat panel.

Parma's team choice has always been to use the panel flat backs as reference flat panels instead of the recommended thin flat panels. As it will be shown below this choice permits to include diffraction phenomena within the reference measurement results.

Both of the measured uniformity diffusion coefficient graphs in figure 10 have two maxima at low frequencies: there is a good correlation between the coefficient maxima frequencies (Fmax) and the panel's dimensions translated to frequency (f1 and f2), considering them as quarter wavelengths.

The measured values actually show an effect on a larger band as expected, since sound interacts with objects in a smeared frequency band around the calculated one.

Panel name	Width [mm]	f1 [Hz]	Depth [mm]	f2[Hz]		F max1	F max2
Single reference	720	119.4	260	330.8		80-160	315-400
Double reference	1440	59.7	260	330.8		50-100	315-400

Table 1

The results show that diffraction can be assimilated to a point-source-like emission of reflection, it is more intense in the smaller panel (higher d values) as expected by a smaller source.

At mid-frequencies the second maximum can be linked to the panel's depth. This relates to the QRD case, where the maximum well depth is considered important for assessing the beginning of the diffusion phenomena in the frequency domain, defining its design frequency [10].

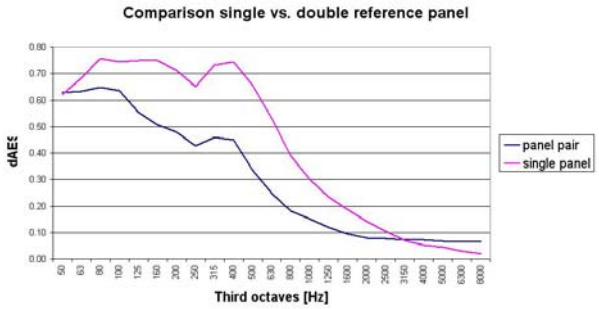

Figure 10.

Figure 11 shows the polar plots for the single flat panel for a normal sound incidence: it is clear that the energy spreading of the reflection can be defined omnidirectional until the 500Hz octave. This happens for all of the angles of incidence and is also stated by the random incidence coefficient values in figure 10: in both graphs the lines begin to drop significantly from the 500 Hz third octave frequency upwards.

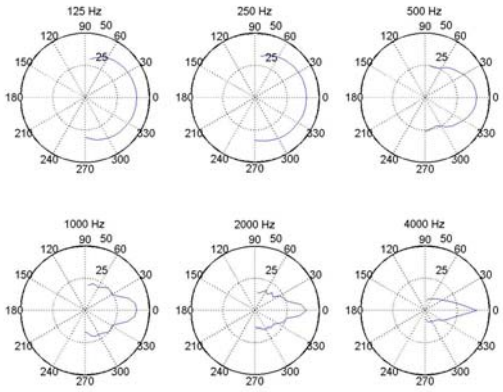

Figure 11.

Comparing the campaign results on single and double panel in figure 10 it is also notable that as the flat reflecting surface widens the reflection coefficient decreases as expected, since it resembles more to an ideal 'acoustical mirror'. This double panel is to be used as a reference, to be compared with all of the following double panel measurements.

Studying the results it is clear that the geometrical limits of the experimental setup impose a never ideal result: low coefficient values can actually be measured only at high frequencies.

The present study on deep panel backs introduce the measurement of a different phenomenon from diffusion: diffraction, which is closely related to it in the mid and low frequency regions [11].

3.2.2 Quadratic Residue Diffuser (number 7).

The calculated coefficient tends to decrease at doubling the panels (figure 12), as seen with the reference panels. It is interesting to recognize the maxima, related to the panel width, very clear the one for the single panel (60 cm wide) at about 200 Hz, less marked the 100 Hz for the QRD7® pair (but still getting near the double flat panel value): it appears that the panel's varying depth surface influences this different behaviour.

Both the graphs have a maximum of diffusion uniformity between 400 and 500 Hz, which correspond to the panel's maximum well depth and its design frequency: these values are almost unvaried by the panel doubling They are not distant in frequency from the reference panels' one: these panels were deeper and with a higher mass density and they showed a coincidence of the second maximum frequency.

The other diffusion increases are parallel in the two measurements: between 1250 and 1600 Hz, corresponding to the wells' width, and the last one is present at 5000 Hz.

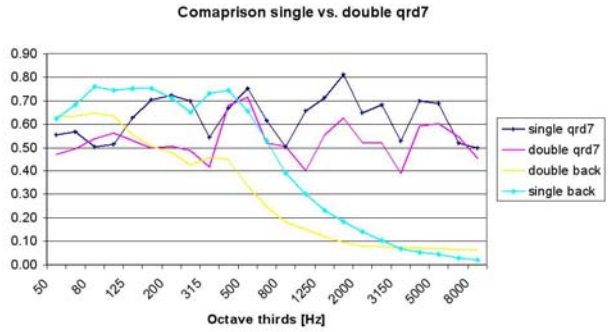

Figure 12.

3.2.3 Galav panels.

The last pairs to be discussed are two 1999 Parma developed Galav1 and Galav2 diffusor panels.

Since they are not symmetrical respect to their front face vertical axis, two possible pairing combinations were studied for each panel type. Figure 13 shows two galav2 in the b configuration while being measured.

Figure 13.

The results were compared with the reference double flat panel, which always was the back side of two paired galav1: the panels show a good diffusion uniformity (figures 14 and 15).

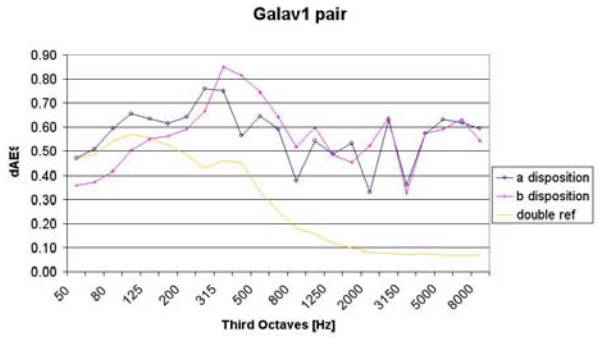

Figure 14.

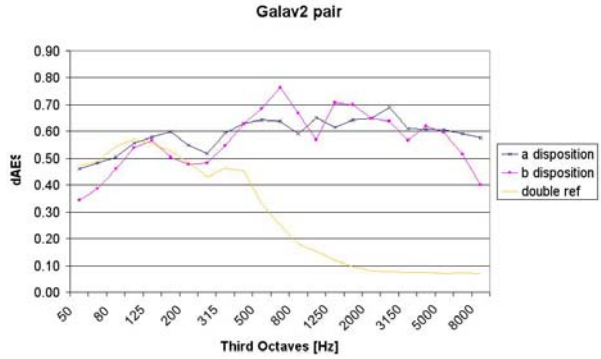

Figure 15.

The results are quite similar for both combinations at high frequencies but oscillate at low and middle ones.

Both the dispositions' results confirm that the designer's intention to lower the functioning bandwidth limits was well obtained: in the Galav1 pair the diffusion uniformity maxima are positioned at less than 315 Hz, less than the panel-depth related frequency as discussed in the past paragraphs.

The Galav2 panels have a quite high and uniform diffusion across the spectrum, expecially in the a disposition.

3.2.4. Comparison between four panel pairs.

Figure 16 compares the studied four panel pairs diffusion uniformity: as already seen the Galav2 pair in disposition (a) has the best result in terms of uniformity of diffusion.

It is also notable that Galav1 has an intentional design frequency which is lower than the QRD7® under test: it is clearly well diffusing as low as at about 250 Hz.

The proposed interpretation of giving diffraction meaning to the coefficient low frequency maxima works well throughout the different typologies, remembering that the apparent width changes in the vertical well-shaped panels and that the Parma developed Galav panels purposely and successfully challenge this physical phenomenon.

These considerations partially question the 'diffusion bandwidth' definition of the recommendation document (par. 3.1.6.) since the low frequency bands are related to the phenomenon of diffraction.

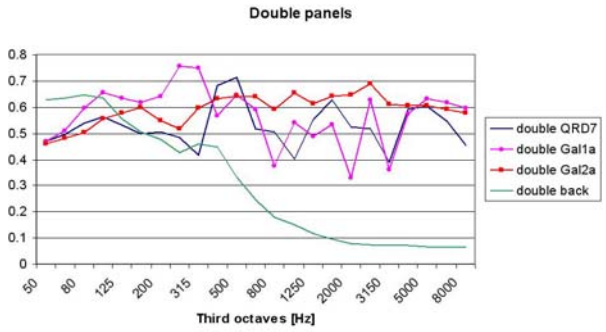

Figure 16.

3.3 Perforated panel's diffusion uniformity.

One single flat perforated 560 x 960 mm panel was measured in two configurations: standing and laying on its side. It had a 1,33% of perforation with a design resonance frequency of about 120 Hz.

Comparing the uniformity diffusion coefficients with the two back panel results (figure 17) it is still notable a decreasing in frequency of the first maximum with increasing panel width (specified in the figure legend in centimeters).

The second maximum is not well defined in the perforated panels as in the reference panels measurements: this should be attributed to the front panel perforation which changes the apparent panel depth to the incising sound, or to an actual emission at lower frequencies, possibly related to the panel's resonant frequency.

The following table shows the quarter wave-length frequencies related to the panel width (f1) and depth (f2) and the frequencies of the main two measured coefficient maxima (Fmax1 and 2). The table confirms that there is a relation between f2 and Fmax2.

It is interesting to note as the perforation appears to give a more peaked trend to the coefficient graph, with an higher maximum value which better relate to a smaller panel respect to the reference panels' behaviour.

More investigations on different perforated panels will permit to confirm these observed trends.

Panel	Width [mm]	f1 [Hz]	Depth [mm]	f2 [Hz]		F max1 [Hz]	F max2 [Hz]
Standing perforated	550	156.4	180	477.8		160-200	400
Laying perforated	924	93.1	180	477.8		100-160	500

Table 2.

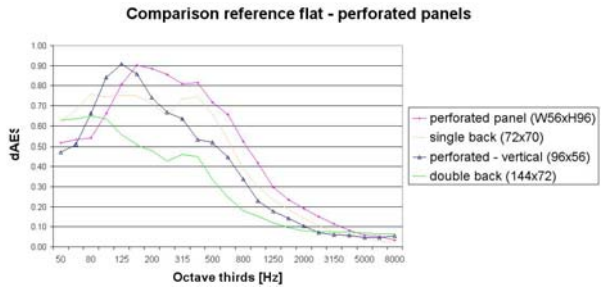

Figure 17.

4. STUDIES OF THE FIRST REFLECTION AND REFLECTIVITY.

The experimental setup is meant to study the first reflection geometry in the emi-space in front of the panel itself: this permitted to move from classical diffusivity considerations and to study the actual first reflection behavior from the perforated panel and then to analyze two possible reflectivity index interpretations.

4.1 Reflection from the perforated panel.

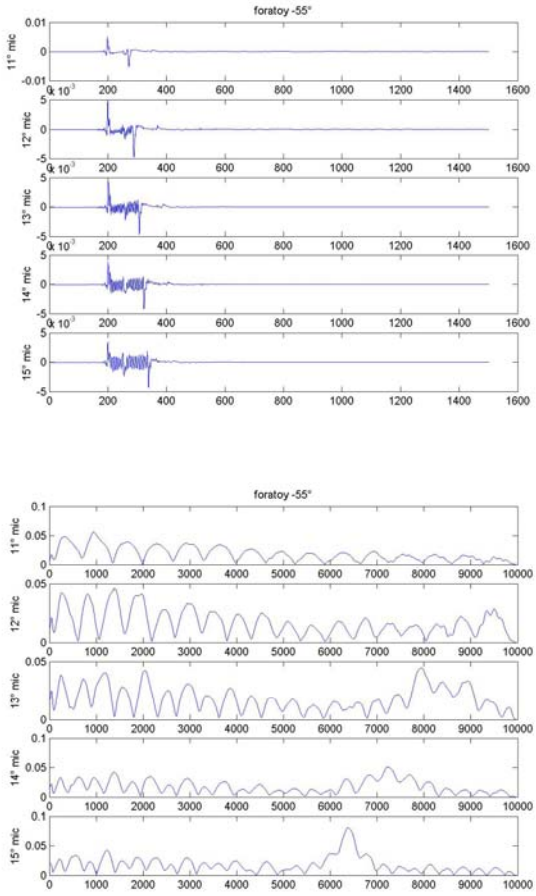

Figures 18a , 18b

An analysis of the single microphone impulse responses showed a strong vibration within the reflection pattern (figure 18a – reflections from the laying perforated panel, with sound incising at -55°, microphone number from 11 to 15), recorded by the microphones in front of the panel when sound was incising laterally.

Lateral microphones (first track shown in figures 18a ,b) recordings were equal to the reference panel measurements, picking up the typical doublet from the panel's edges, this translates into a well defined comb effect in frequency.

These considerations led to study the relative frequency responses in detail (figure 18 b): this showed that the phenomenon is always localized in narrow bands and that it shifts in frequency depending on the angle of observation.

In the discussed case of the horizontal disposition of the panel it is localized only in a specific sector of the emi-space and presents an inversion at about 45° (table 3), when the panel was measured in the vertical position it is more spatially limited (37.5° wide instead of 90° as seen in the next table).

FORATOY – 55°		
Mic #	**Fmax**	**Theta**
12	9.50E+03	-7.5
13	**7.95E+03**	**0**
14	7.23E+03	7.5
15	6.38E+03	15
16	5.77E+03	22.5
17	5.25E+03	30
18	4.83E+03	37.5
19	*4.57E+03*	*45*
20	*8.65E+03*	*52.5*
21	8.27E+03	60
22	7.97E+03	67.5
23	7.78E+03	75
24	7.70E+03	82.5

Table 3.

It was decided to compare the phenomenon with sound radiation from loudspeaker arrays when fed on a regular delay line. The panel was hence modeled as a matrix of monopole sources [12], positioned and with the same radius as the panel holes, it was studied their contribute at each point on the observation semicircle Each omni-directional source was considered emitting sound on the moment the incising sound illuminated it: the result of an accurate model are shown in figure 19.

Equation 5 shows the equation describing the model with a two dimensional sum and a separate propagation contribution.

$$p = \frac{\rho_0 kc(4\pi a^2 \hat{u})}{4\pi \cdot r} \sum_i \sum_j e^{-jkx_{i,j}} e^{-jky_{i,j}} \quad (5)$$

where:

a = source radius (hole radius)
u = superficial velocity module = 0.1 m/sec
r = reception array distance = 5 m
i = i-th matrix column
j = j-th matrix row
$x_{i,j}$ = distance between illuminating source and each monopole (panel's holes - emission delay)
$y_{i,j}$ = distance between each monopole and the receiving array (1000 points of reception)

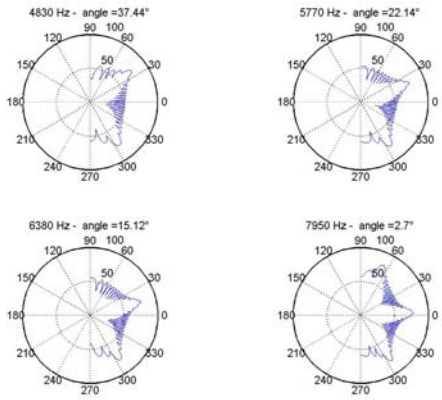

Figure 19.

The model results in figure 19 on the specific frequencies, taken from table 3, give a good angular match with the measurements of table itself: the same promising results are obtained modeling the vertically positioned panel.

These results confirm the existence of a natural re-irradiation phenomena from the hole sequence which deserves further research on its modifiability and perceptibility.

4.2 Reflectivity study through time-normalized impulse responses.

An approach similar to EN 1793-5 [13] was attempted to the data: this measurement standard uses time normalized reflected and incident sound impulse responses to calculate a reflection coefficient for noise attenuating road barriers by dividing pseudo intensity values.

$$RI_j = \sum_{k=1}^{n_j} \frac{\int_{\Delta f_j} \left| F\left[t \cdot h_{r,k}(t) \cdot w_r(t) \right] \right|^2 df}{\int_{\Delta f_j} \left| F\left[t \cdot h_{i,k}(t) \cdot w_i(t) \right] \right|^2 df} \quad (6)$$

j j-th third octave frequency band
k number of microphone (observation angle)
$h_{r,k}$ reflected wave impulse response
$h_{i,k}$ incident wave impulse response
t time (normalization parameter)

A first analysis on the time-normalization process (multiplication of each track by time - figure 20) illustrates how the semi-circular shape of the array and the limited dimension of the panels give importance to the energy reflected by the borders and the sides of the panel themselves.

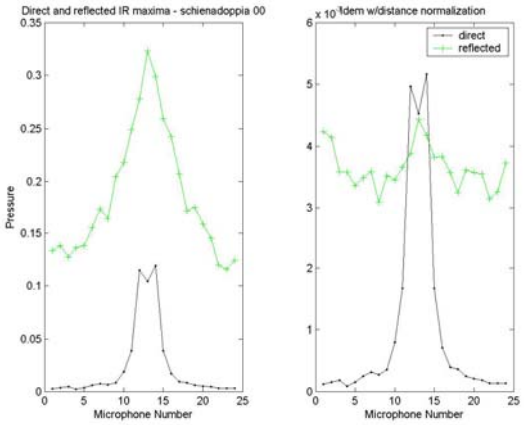

Figure 20.

The first calculations based on equation 6 gave small values (never passing 2%): this is correlated to the fact that the measurement array measured more incident energy than the one actually hitting the panel.

So it was decided to divide the reflected pseudo-intensity values by the summation of the incident pseudo-intensities measured just by the microphones within the incidence cone on the panel, and to average the measurements on the various angles of incidence to obtain a 'random' value.

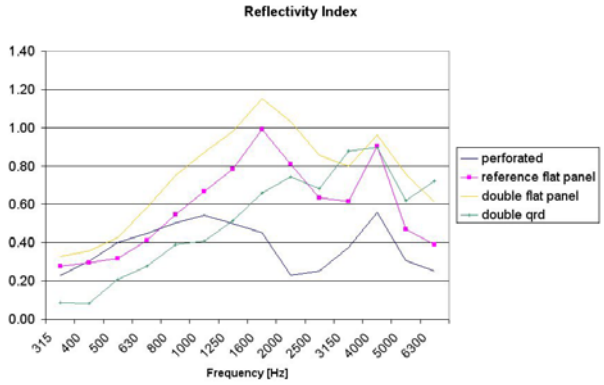

Figure 21.

The result is clearly not the energetic reflection coefficient as measured in a reverberation chamber, there is no randomisation of incidence as in more modern intensity based measurements techniques [14]. Actually small specimens are not permitted by the cited European standard that requires large barriers and small distances of observation.

The parameter could be defined as a 'cylindrical reflectivity index': a datum that still permits to compare the various panels within the same experimental setup and to obtain a first estimation of their absorption behaviour in frequency, expecially in the plane of analysis. The main advantage is that these values can be easily obtained together with the uniformity diffusion coefficient.

The results in figure 21 are actually in line with the panels' well known behaviours: they show that in the mid and high frequency regions the reference panels are the most reflective, the double qrd have the best absorption at mid frequencies, while the perforated panel tend to absorb mostly at mid and high frequencies.

Low frequencies were not considered because of diffraction which strongly influences this type of measurement, making them quite similar.

4.2 Reflectivity analysis through fitting of a theoretical model.

As discussed in a second 1999 paper from Parma's team [15], the experimental data were used to fit a theoretical model of reflection, so to extract diffusion coefficients that can be used in an acoustical modeling software [16].

$$I_{diff} = \int_{y=-b}^{b} \int_{x=-a}^{a} \frac{W \cdot z_c}{4\pi \cdot r_1^3} \cdot \frac{(1-\alpha) \cdot \delta_{loc}}{2\pi \cdot r_2^2} dx \cdot dy \quad (7)$$

where:

W the source's power
Zc the distance between source and the centre of the panel
R1 the distance between the source and the a*b portion of the panel
R2 the distance between the small portion and the receivers
α the absorption coefficient

δloc is the computer program diffusion coefficient which increments to 1 as the surface particle in exam gets near the panel's border

$$\delta_{loc} = 1 - (1-\delta)\frac{2 \cdot d_{\min}}{\lambda} \quad \text{eq. 8}$$

Each panel surface was divided into a 11x11 a*b surface-particle matrix and the analytical computation was performed numerically using the Excel spreadsheet. Fitting the value of W on the filtered measurement pseudo intensity data, the solver function was used to automatically optimise α and δ to maximally match the reflected pseudo intensity values.

In the present study the observation array was quite different from the past one, at the time it was a synthetic linear array of 255 closely spaced points, giving a narrower span but more precise angular resolution.

First analysis on the single reference panel gave good fitting at 2 KHz with past results on single panels (δ = 0.114), although the experimental intensity values outside the specular region often over-ranged the theoretical ones. The different type of source, the different angular resolution, suggest to repeat the experiment on single panels and to continue research on the matter.

The results appear promising to use the standard geometry setup to acquire data for the Ramsete modelling software, expecially at high frequencies.

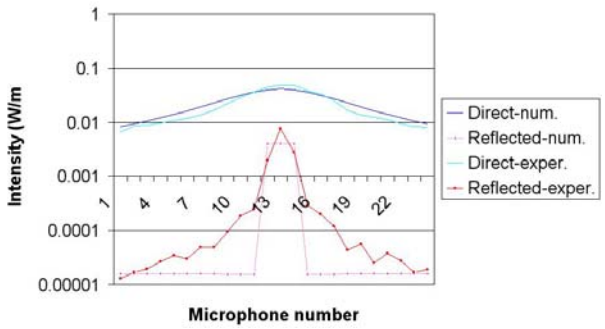

Figure 22.

5. CONCLUSIONS.

The continuation of data elaboration permitted to investigate into more detail the sound scattering phenomena from the spatial distribution point of view, using some standard conceptual devices and introducing some innovative considerations and questions.

A smaller geometry measurement setup permitted to understand new possibilities to study sound focusing.

The standard measurement setup and data elaboration permitted to enlarge the diffusion concept to lower frequencies defining it as diffraction, to study a perforated panel interesting behaviour and to investigate on panels' reflectivity from two diverse points of view.

Most of the discussions that were begun here need further exploration and research, but they open interesting debating points and suggestions to the AES-4id recommendation document renovation process, expecially for the more economic use of large not anechoic spaces as the one used for these studies.

6. ACKNOWLEDGEMENTS

LAE [12] wishes to thank Ing. Alfieri and Fiere di Parma for permitting the use of the large space needed for the experiments.

7. REFERENCES

[1] Lorenzo Rizzi, Angelo Farina, Paolo Galaverna et Al. , Surface scattering uniformity measurement in reflection free environments, 121st AES Convention,

San Francisco, 5-8 October 2006 , Convention Paper 6922

[2] AES-4id-2001, AES information document for room acoustics and sound reinforcement systems - Characterization and measurement of surface scattering uniformity.

[3] Peter D'Antonio, Trevor Cox, Two decades of sound diffusor design and development. Part 1 and 2, JAES Volume 46 Number 11-12 pp 955-976; 1075-1091 November-December 1998

[4] Peter D'Antonio, The Directional Scattering Coefficient: Experimental Determination, JAES Volume 40 Number 12 pp. 997-1017, December 1992.

[5] Angelo Farina, Michele Zanolin, Elisa Crema, Measurement of sound scattering properties of diffusive panels through the Wave Field Synthesis approach, 108th AES Convention, Paris 18-22 February 2000.

[6] Angelo Farina, Measurement of the surface scattering coefficient: comparison of the Mommertz/Vorländer approach with the new Wave Field Synthesis method, International Symposium on Surface Diffusion in Room Acoustics - Liverpool (GB) 16 April 2000.

[7] Angelo Farina, Lorenzo Rizzi, Comments on reaffirmation AES-4id-2001 http://www.aes.org/standards/b_comments/comments-reaffirm-aes-4id.cfm

[8] Lorenzo Rizzi, Angelo Farina, Paolo Galaverna et Al., Study of scattering panel pairs in virtually anechoic environments . 19th International Congress of Acoustics.

[9] Angelo Farina, Simultaneous Measurement of Impulse response and distortion with swept sine technique, 108th AES Convention, JAES (Abstracts) volume 48 p 350, April 2000, preprint 5093

[10] F.A. Everest, The master handbook of acoustics, McGraw Hill, 4th edition

[11] Arthur Noxon, Correlation Detection of Early reflections, 11th AES International Conference, April 1992

[12] L. Kinsler, A. Frey, A. Coppens, J. Sanders, Fundamentals of Acoustics, John Wiley and sons, 4th edition

[13] EN 1793 - 5 Road traffic noise reducing devices - Test method for determining the acoustic performance - Part 5: Intrinsic characteristics - In situ values of sound reflection and airborne sound insulation

[14] Michael Voerlander, Eckard Mommertz, Definition and measurement of random incidence scattering coefficients, Applied Acoustics 60 (2000) 187-199

[15] Angelo Farina, Introducing the surface diffusion and edge scattering in a pyramid tracing numerical model for room acoustics, 108th AES Convention, Paris 18-22 February 2000.

[16] Ramsete - Room acoustic modelling on PC – www.ramsete.com